$Na_{1/2}Bi_{1/2}TiO_3$-based lead-free piezoceramics: a review of structure–property correlation

Rajeev Ranjan*

Department of Materials Engineering, Indian Institute of Science, Bengaluru 560 012, India

Piezoelectric materials transform electrical energy to mechanical energy and vice-versa making them technologically important as actuators, sensors and transducers in wide ranging applications. New regulations on prevention of hazardous materials in industrial applications have led to a great surge in research on environment friendly alternatives of the commercial Pb-based piezoelectrics – Pb(Zr, Ti)O_3. The field of lead-free piezoceramics has seen great advances in the last two decades. This review focuses on the current status of understanding of structure–property relationships in $Na_{1/2}Bi_{1/2}TiO_3$-based lead-free polycrystalline piezoceramics.

Keywords: Materials, piezoceramics, structure–property relationships.

THE phenomenon of piezoelectricity, wherein a material develops voltage on application of mechanical force (direct piezoelectric effect) and changes dimension on application of electric field (converse piezoelectric effect), was discovered by Curie brothers in 1880 in single crystalline quartz minerals[1]. Piezoelectric materials are currently being used in wide ranging applications such as transducers, actuators, pressor sensors, mechanical energy harvesting[2]. The most common parameter to characterize a piezoelectric material is the piezoelectric coefficient (d) defined as the ratio of strain and electric-field (for the converse phenomenon) or ratio of polarization and stress (for the direct phenomenon). The piezoelectric coefficient d is commonly represented in units of pico-Coulomb/Newton (pC/N) for the direct-effect and picometre/Volt (pm/V) for the converse effect. Both units are thermodynamically (and dimensionally) equivalent[3]. The piezoelectric coefficient d is a third rank tensor and has a maximum of 18 independent components. According to the Neuman's principle, all the components are zero for a crystalline material, the structure of which has a centre of inversion symmetry. A fundamental requirement for a material to exhibit piezoelectricity is that its crystal structure should exhibit non-centrosymmetric point group. Among the 32 crystallographic point groups, 20 of them can show piezoelectric effect[3].

*e-mail: rajeev@iisc.ac.in

The piezoelectric coefficient of a single crystal quartz is 2 pC/N (ref. 4). Research on piezoelectric materials picked up after the discovery of ferroelectricity in $BaTiO_3$ during the Second World War[5]. Ferroelectrics, first discovered in Rochelle salt in 1921 (ref. 5), are a sub-class of piezoelectrics exhibiting spontaneous polarization, the direction of which can be reoriented by application of a strong electric field. Once subjected to a sufficiently strong electric field, the remanent polarization of a ferroelectric material makes it possible even for polycrystalline ferroelectric ceramic to behave as a piezoelectric-material. Polycrystalline ceramics are easy to synthesize compared to single crystals and are attractive for mass scale production[6]. A polycrystalline $BaTiO_3$ ceramic shows a longitudinal piezoelectric coefficient d_{33} (polarization measured along the axis of the applied force) ~190 pC/N (ref. 6) which is considerably larger than the piezoelectric coefficient of a single crystal quartz. However, after the discovery of better piezoelectric properties in pseudo-binary system $PbTiO_3$–$PbZrO_3$ (commonly abbreviated as PZT)[6], interest in $BaTiO_3$-based ferroelectrics shifted towards the development of high dielectric constant materials[7]. Though ferroelectricity is known in many different families of inorganic and organic materials, the ABO_3 oxide ferroelectric perovskites have attracted most attention because of their significantly large piezoelectric properties. The highest symmetry phase of a perovskite structure is cubic (space group Pm-3m). Being centrosymmetric, this phase is paraelectric. On cooling below the Curie point (ferroelectric–paraelectric phase transition temperature), the paraelectric state transforms to a ferroelectric state along with a concomitant change in the crystal structure. For example, $BaTiO_3$ is paraelectric with a cubic structure above 130°C. Below 130°C, it transforms to a tetragonal (space group P4mm) ferroelectric phase. The spontaneous polarization in the tetragonal phase is along the [001] direction, i.e. parallel to the c-axis. On cooling further, $BaTiO_3$ undergoes two more structural transitions: orthorhombic ferroelectric phase (space group Amm2) with spontaneous polarization parallel to [110] direction and rhombohedral ferroelectric phase (space group R3m) with spontaneous polarization parallel to [111] direction[6]. These directions are referred to with respect to the pseudocubic unit cell.

For over five decades, PZT-based piezoceramics have been the material of choice in most commercial

applications. The importance of PZT is not only because of its large piezoelectric response but also because of good thermal stability of the piezoelectric properties. It derives this unique feature from the composition–temperature phase diagram which exhibits a nearly vertical morphotropic phase boundary (MPB) at ~52 mol% of $PbZrO_3$. The MPB of PZT separates rhombohedral and tetragonal phase fields[6,7] and is therefore a composition driven inter-ferroelectric instability. This instability causes near flattening of the free-energy profile making it easy for the polarization to rotate on application of external electric-field and/or mechanical stress[8] – the intrinsic piezoelectric response. The inter-ferroelectric instability also reduces the energy of the domain walls significantly, allowing their density and mobility to increase – the extrinsic contribution to piezoelectricity[9,10]. The discovery of considerable enhancement of the electromechanical response at the MPB in PZT has guided subsequent exploration of compositional engineering in other ferroelectric solid solutions.

Lead-free piezoceramics

In the past two decades increased environmental concerns and introduction of regulations aimed at restricting the use of toxic materials in industrial applications[11] have oriented the scientific community to focus on Pb-free piezoelectrics[12–21]. The first breakthrough that accelerated research on Pb-free piezoelectrics, was the discovery of large piezoelectric effect ($d_{33} \sim 450$ pC/N) in textured ceramic of Li, Ta modified $K_{0.5}Na_{0.5}NbO_3$ (KNN)[22]. Over the period, higher d_{33} (~500 pC/N) has been reported even in non-textured KNN-based ferroelectric systems[23]. Like the MPB in PZT, the compositional modification of KNN (by Li, Ta, Sb) is aimed at pushing the system towards an inter-ferroelectric instability at room temperature[24–29]. As with $BaTiO_3$, $KNbO_3$ (and KNN) exhibits the same sequence of structural transitions on cooling from high temperature: cubic (paraelectric) → tetragonal (ferroelectric) → orthorhombic → rhombohedral (ferroelectric). Analogous scenario in $BaTiO_3$ can be achieved by substitution of Zr, Sn and Hf at the Ti-site, leading to enhancement in the piezoelectric response from ~190 pC/N (unmodified $BaTiO_3$) to ~400 pC/N in the modified systems[25,26]. Interestingly, although the phase diagram is nearly the same, a notably larger d_{33} (~600 pC/N) was reported in Ca-modified Ba(Ti, Zr)O_3 (ref. 28), Ca-modified Ba(Ti, Sn)O_3 (refs 29–31) and Ca-modified Ba(Ti, Hf)O_3 (ref. 32) systems. Despite their large piezoelectric coefficient, $BaTiO_3$-based piezoelectrics have the drawback of low Curie point ($T_c \sim 80$°C). This makes the system vulnerable to thermal depoling and deterioration in the piezoelectric response due to any unintentional increase in the temperature of the device during operation. In this context, though the KNN-based piezoelectrics are preferred because of their higher Curie point, their major drawback is the large dependence of the properties on the synthesis conditions. $BiFeO_3$ is another interesting lead-free ferroelectric compound with very high Curie point (~800°C)[33]. Synthesis of pure $BiFeO_3$ is however difficult under normal conditions due to the presence of competing non-perovskite phases in the Bi_2O_3–Fe_2O_3 phase diagram[33]. Another problem with $BiFeO_3$ is the large leakage current which makes poling difficult. These issues are resolved to a certain extent in solid solutions of $BiFeO_3$ with other perovskites[34–36]. Some solid solutions of $BiFeO_3$ show reasonably high d_{33} (~324 pC/N)[34] together with a high Curie point of 466°C, making them interesting for high temperature applications. One of the most extensively studied lead-free piezoelectric systems are based on the solid solutions of $Na_{0.5}Bi_{0.5}TiO_3$ (NBT) – sodium bismuth titanate. An important highlight of NBT-based piezoelectrics is the large electrostrain (~0.7%) at ~60 kV/cm making them interesting for high performance actuator applications[37,38]. Because of the ease of synthesis, reproducibility of properties, and moderate depolarization temperature, NBT-based lead-free piezoelectrics have been preferred in high-power ultrasonic devices[17]. The complexity of the microstructure and crystal structure however, pose a great challenge for establishing structure–property relationships in NBT-based piezoceramics. Further in this review, a survey of the work with focus on structure-property correlations in NBT-based piezoceramics is presented.

$Na_{0.5}Bi_{0.5}TiO_3$ (sodium bismuth titanate)

$Na_{0.5}Bi_{0.5}TiO_3$ (NBT) was discovered in 1961 by Smolensky *et al.*[39] as a rhombohedral (space group *R*3*c*) ferroelectric perovskite. NBT shows remnant polarization $P_r = 38$ μC/cm^2, coercive field in the range 50–60 kV/cm, $d_{33} \sim 70$ pC/N and Curie point 320°C (the temperature corresponding to permittivity maximum). The temperature dependence of dielectric constant of NBT exhibits two anomalies – a broad maximum at 320°C and a hump at ~200°C (refs 37–48). The hump at 200°C exhibits considerable frequency dispersion suggesting a relaxor ferroelectric behaviour[43,44]. Many reports exist on the anomalous changes in the physical properties of NBT in the temperature region 200–300°C (ref. 44). On heating, the remanent polarization decreases dramatically at 200°C, the depolarization temperature[44]. The intermediate phase between 200°C and 320°C exhibits a pinched P–E hysteresis loop, a feature attributed to the onset of an anti-ferroelectric phase[40]. However, neutron diffraction studies did not reveal any signature of anti-ferroelectric structure[49]. In contrast to common ferroelectrics like $BaTiO_3$, $PbTiO_3$ or $KNbO_3$, the paraelectric phase exhibits a cubic (Pm-3m) structure, the paraelectric phase of NBT is a non-cubic tetragonal (space group P4bm)

structure comprising of in-phase tilt of the neighbouring octahedra along the *c*-axis of the tetragonal cell[50]. The cubic (Pm-3m) phase appears at higher temperature (~520°C)[51]. Cordero *et al.*[52] reported sharp anomalies in the elastic compliance of NBT at ~550°C and 290°C and did not find any special structural origin of thermal depolarization at ~200°C. The two anomalies were attributed to the ferroelastic cubic (Pm-3m) – tetragonal (P4bm), ferroelectric P4bm–*R*3*c* transitions respectively. NBT exhibits a complex evolution of domain pattern in the temperature range 200–300°C, comprising of extensive twinning and formation of an intermediate orthorhombic (Pnma) structure on a shorter length scale[53,54]. The pinched P–E loop in this temperature region is attributed to this structural heterogeneity.

Structural disorder in NBT at room temperature

NBT exhibits a considerable degree of structural–polar disorder at room temperature. Balagurov *et al.*[55] reported that the residue of the high temperature P4bm phase is found even at room temperature leading to an incommensurate modulation of the octahedral tilt. Evidence of long-period modulation in NBT was also reported by Thomas *et al.*[56] using X-ray diffuse scattering study. Earlier, Kriesel *et al.*[57] reported the existence of local monoclinic displacement of the Na/Bi ion. Neutron pair distribution function study of NBT by Keeble *et al.*[58] suggested a bifurcated polarization due to two distinctly different polar displacement of Bi^{+3}. First principles studies have revealed a complex interaction between local A-site cation ordering and octahedral tilt, and its influence on the relaxor ferroelectric behaviour of NBT[59–61]. The fundamental origin of the inherent structural disorder in NBT lies in the qualitatively different bonding characteristics of the Na–O (primarily ionic) and Bi–O (primarily covalent) bonds. Local structure studies by extended X-ray absorption fine structure (EXAFS) have revealed that the Bi–O bonds are 0.3 Å shorter than that revealed by structural analysis of X-ray/neutron diffraction data[62,63]. This confirms that the local environment of Bi is much distorted from that anticipated based on the average global structure. Aksel *et al.*[64] have shown the structure when probed on the length scale of less than 10 Å to be different from the average structure as seen by diffraction techniques. A readjustment of the Bi–O bond distance was noted in poled specimen of NBT but not in the Ti–O distances, suggesting that strong electric field induces a correlated motion between the Bi-off centering and octahedral tilt[63]. ^{23}Na and ^{49}Ti nuclear magnetic resonance (NMR) spectroscopy studies have also revealed disorder on the A and B sites of NBT[65,66], consistent with the other local structure studies.

The structural disorder on the local scale have a profound effect on the average structure perceived on the global scale. Gorfman and Thomas[67] and Aksel *et al.*[68] reported that the conventional rhombohedral (*R*3*c*) structural model was not enough to account for all the features of the high-resolution X-ray diffraction data of NBT. They proposed a monoclinic structure in the space group *Cc*. Levin and Reaney[69] explained average monoclinic *Cc* structure in terms of assemblages of orthorhombic (average octahedral tilt $a^-a^-c^+$) domains comprising of in-phase tilted octahedral region of few nano metres and comparatively longer antiphase tilted regions[69]. Rao *et al.*[70] have shown signatures of Bragg peaks corresponding to *R*3*c* and *Cc* phases in high resolution synchrotron X-ray diffraction patterns of NBT (Figure 1). The relative fractions of the two phases are very sensitive to the treatment of the specimens by external electric-field and mechanical stress[71,72]. A correlation between the average *Cc* structure and high density of twinning was reported by Beanland and Thomas[72]. The regions in the specimen with less density of defect appear as rhombohedral[72]. Rao and Ranjan[71] showed that poling of the NBT almost suppresses the monoclinic (*Cc*) phase and makes the global structure appear rhombohedral (*R*3*c*) (Figure 1). This is accompanied by suppression of the in-phase tilted local regions[45] (Figure 1), and readjustment of the displacements of the Bi cation in conformity with the long-range rhombohedral structure[62,73]. Recently, it was shown that even the monoclinic *Cc* average structure of NBT changes to cubic when the grain size is reduced to ~2 microns[74]. Strong electric field could however bring about a cubic to rhombohedral distortion[74]. These studies confirm that the appearance of the different global structure cubic/monoclinic in the unpoled state of NBT is not associated with a structural transformation on the scale of unit cell but manifestations of different types of assemblages of the in-phase and anti-phase tilted regions[69]. In this context, Aksel *et al.*[68] have shown that the local deviations from the average structure is more in the calcined NBT (smaller grain size) as compared to their sintered counterpart (larger grains).

Off-stoichiometry studies

Owing to the strong influence of structural disorder on the average structure and properties, it is anticipated that chemical modifications of NBT, including making it off-stoichiometric, would strongly influence its structure and properties[75–85]. Li *et al.*[85] reported large oxygen ion conductivity in A-site off-stoichiometric NBT compositions. In general, Na-excess/Bi-deficient compositions decrease and Na-deficient/Bi-excess increase the resistivity[75,78,84]. Some reports show enhancement in piezoelectric response and lowering of the depolarization temperature in Bi-excess/Na-deficient compositions of NBT[75,78,79,81]. A detailed study on the effect of off-stoichiometry on the grain size, structure, electrical conductivity, impedance,

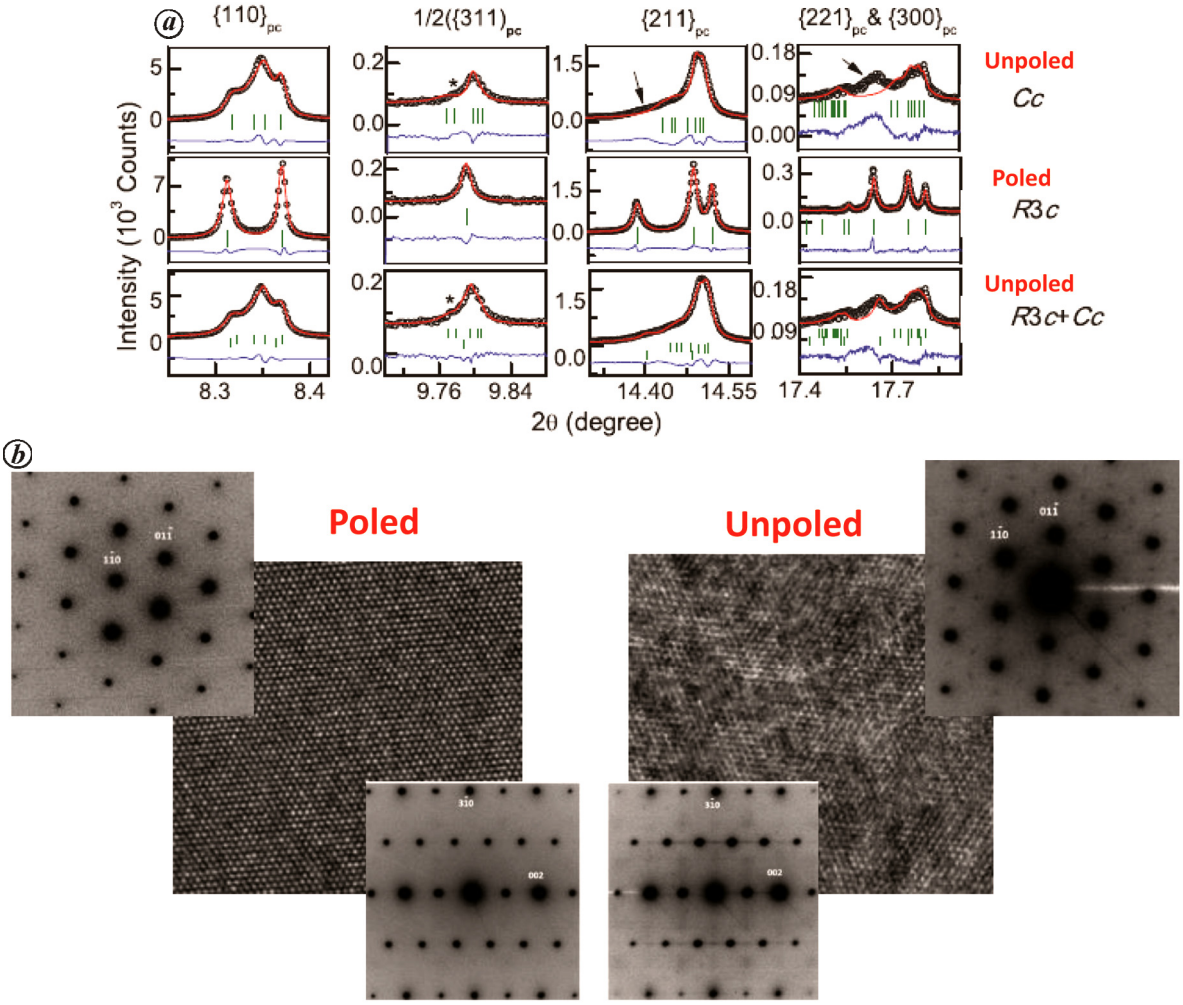

Figure 1. ***a***, Selected profiles of the whole pattern Rietveld fitted high-resolution synchrotron X-ray (wavelength = 0.39991 Å) powder diffraction pattern of unpoled and poled $Na_{0.5}Bi_{0.5}TiO_3$ specimens. The diffraction pattern on the poled specimen was recorded after breaking the poled pellet to powder to avoid preferred orientation effect. For the unpoled specimen the ground powder obtained from pellet was annealed at high temperature to get rid of stress induced structural changes. The arrows in the first row show unaccounted Bragg peaks corresponding to the rhombohedral phase when the data was fitted with monoclinic (*Cc*) phase. The patterns in the second row shows pattern of poled NBT fitted with single phase *R3c* structural model. All features in the diffraction pattern of the unpoled specimen are nicely accounted for with the *Cc* + *R3c* phase coexistence model as shown in the third row. ***b***, The HRTEM and electron diffraction patterns of unpoled and poled NBT corresponding to [111] (shown at top corners of the corresponding HRTEM image) and [130] (shown at the bottom corners of the corresponding HRTEM image) zone axes. Important to note that the HRTEM of the unpoled NBT is hazy and that of the poled specimen show relatively well defined lattice fringes. The [111] zone axis diffraction pattern of unpoled NBT shows ½{odd odd even} type superlattice spots which are absent in the pattern of poled specimen. Also, diffuse streaks between Bragg spots are evident in the [130] zone axis pattern of unpoled specimen and not in the poled specimen[70].

dielectric, ferroelectric and piezoelectric properties of NBT was recently reported by Mishra *et al.*[75] (Figure 2 *a*, *b*). The d_{33} increased from ~80 pC/N for $x = 0$ to ~100 pC/N for $x = -0.04$ in the off-stoichiometric composition series synthesized as per the chemical formula $Na_{0.5}Bi_{0.5+x}TiO_3$ (Figure 2 *b*). Mishra *et al.*[75] reported a correlation between off-stoichiometry, grain size and d_{33}. Structural analysis of the poled specimens of the different off-stoichiometric compositions revealed a consistent increase in the degree of structural disorder with increasing Na-deficiency and Bi-excess specimens. The off-stoichiometric composition exhibiting the best piezoelectric response has an optimum fraction of the structural disorder coexisting with the field stabilized long-range ferroelectric order[75]. A similar trend was reported with grain size of stoichiometric NBT[74] and led the authors to argue that perhaps, in addition to the chemistry, comparatively reduced grain size in Na-deficient/Bi-excess off-stoichiometric NBT has a role to play in increasing the piezoelectric response[74,75] (Figure 2 *c*).

NBT-based solid solutions

As stated above, the common compositional design approach in ferroelectric materials to enhance the piezoelectric

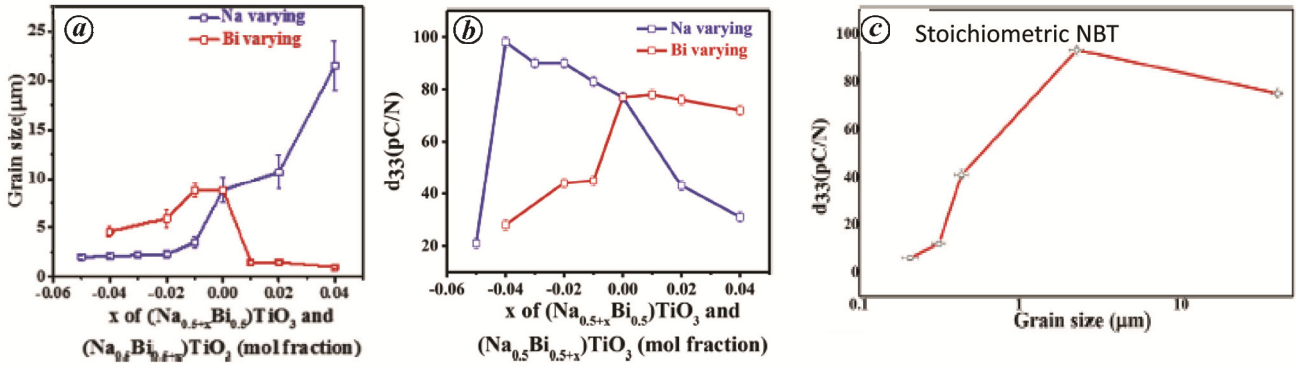

Figure 2. ***a***, The grain-size dependence as a function of off-stoichiometry in $Na_{0.5+x}Bi_{0.5}TiO_3$ (blue) and $Na_{0.5}Bi_{0.5+x}TiO_3$ (red). ***b***, The dependence of longitudinal piezoelectric coefficient (d_{33}) on the extent of off-stoichiometry for the two series. Note the considerable increase in the piezoelectric coefficient for the off-stoichiometric composition $Na_{0.96}Bi_{0.50}TiO_3$. ***c***, The piezoelectric coefficient as a function of grain size for stoichiometric NBT. The specimen with grain size ~2 μm shows better d_{33} than that of the higher grain size[74,75,84].

response is to induce an inter-ferroelectric instability at room temperature. Given that NBT is a rhombohedral (*R*3*c*) ferroelectric, it is anticipated that if it is modified by another ferroelectric perovskite compound with tetragonal structure, a composition driven rhombohedral-tetragonal inter-ferroelectric instability can be induced. Over the years, this strategy has been tried by researchers, an extensive compilation of which can be found in ref. 16. The two most prominent lead-free derivatives of NBT are the pseudo-binaries $(1–x)Na_{0.5}Bi_{0.5}TiO_3$–$(x)BaTiO_3$ (NBT–*x*BT)[86–113] and $(1–x)Na_{0.5}Bi_{0.5}TiO_3$–$(x)K_{0.5}Bi_{0.5}$–$TiO_3$ (NBT–*x*KBT)[114–135]. Both $BaTiO_3$ and $K_{0.5}Bi_{0.5}TiO_3$ are tetragonal (P4mm) ferroelectrics at room temperature and when increasingly dissolved in NBT are expected to show a rhombohedral–tetragonal instability. Takenaka *et al.*[86] reported the first phase diagram of NBT–*x*BT showing a morphotropic phase boundary at $x = 0.06$ separating rhombohedral and tetragonal phase fields. The phase diagram of NBT–*x*KBT with MPB at $x \sim 0.20$ was first reported by Sasaki *et al.*[115]. The MPB compositions of NBT–*x*BT and NBT–*x*KBT show maximum dielectric and piezoelectric properties. The highest reported d_{33} for NBT–BT is 186 pC/N[111] and for NBT–KBT is 207 pC/N[125]. It is important to point out that the maximum reported d_{33} in NBT-based piezoelectrics is significantly less when compared to the highest d_{33} reported in the $BaTiO_3$-based and KNN-based lead-free piezoelectric systems ($d_{33} \sim 550$–600 pC/N). This issue has recently been dealt with by Adhikary and coworkers[132–134], discussed in the next section. In contrast to the classical Pb-based MPB systems like PZT, the MPB composition of which shows a coexistence of tetragonal and rhombohedral/monoclinic phases on the global scale, the MPB compositions of NBT–BT and NBT–KBT exhibit a cubic-like structure[87,91,94,98,132,133]. The signature of the tetragonal and rhombohedral phases can however be seen in the Raman spectra[89] and in the photoluminescence studies[108,110] confirming that, as with the parent compound NBT[69,72,75,84], the cubic like global structure of the MPB compositions of NBT–BT and NBT–KBT is associated with microstructural heterogeneity on a mesoscopic length scale. Similar to NBT, strong electric field induces a cubic to rhombohedral/rhombohedral + tetragonal structures[91,98,104,109,133]. Using the slope of the linear plots between permittivity and log–frequency as an indicator of polar-heterogeneity (Figure 3), Garg *et al.*[93], Khatua *et al.*[109] and Adhikary *et al.*[133] argued that the structure–polar heterogeneity increases, which in turn increases the relaxor–ferroelectric characteristic, as the MPB is approached. These authors have also reported that the system tends to form a long-period modulation in the octahedral tilt configuration suggesting a sequential arrangement of the in-phase and anti-phase tilts[98,133]. Poling, however, dramatically suppresses the in-phase tilts and transforms the structure to rhombohedral or rhombohedral + tetragonal[93,98,133] (Figure 3 *d*). The short ranged relaxor state to long-range ferroelectric transformation has also been reported by mechanical stress[93,136]. The signature corresponding to the long-period modulation persists in the tetragonal (P4mm) composition region ($x > 0.07$) until $x \sim 0.20$. Rao *et al.*[105] have demonstrated evidence of a new criticality at $x = 0.2$ in the $(1–x)$NBT–(x)BT system where the coercivity and the spontaneous tetragonal strain exhibit a non-monotonic dependence with composition well within the tetragonal composition regime (Figure 4). Using neutron diffraction as a tool, Rao *et al.*[105] showed that this new criticality is associated with the system's transformation from a non-modulated tetragonal phase (for $x > 0.2$) to a modulated tetragonal phase (for $x < 0.2$). The occurrence of modulation in the octahedral tilt configuration depolarizes the system well before the diffuse dielectric anomaly temperature, i.e. inducing a relaxor–ferroelectric characteristic to the system.

As stated above, a unique feature of NBT-based piezoelectrics is that some compositional derivatives exhibit large high-field electrostrain compared to

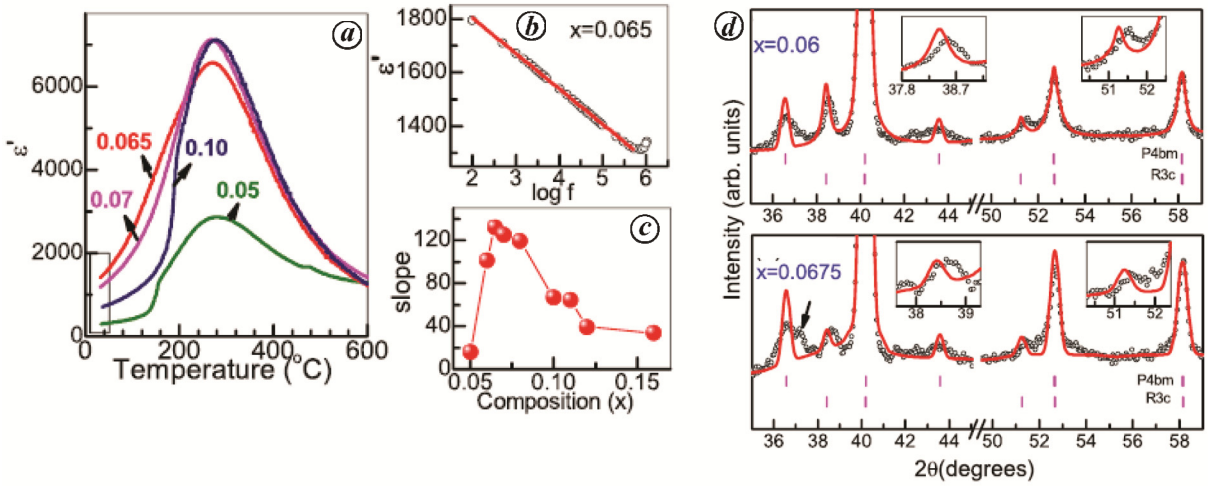

Figure 3. ***a***, Temperature dependence of relative permittivity of $(1–x)Na_{0.5}Bi_{0.5}TiO_3–(x)BaTiO_3$ for different $BaTiO_3$ concentration (x values shown in the plot). ***b***, The permittivity as a function of log-frequency for a representative composition $x = 0.065$ (in the MPB region) measured at room temperature. The slope of the such plots as a function of $BaTiO_3$ concentration (x) is shown in (***c***). Important to note that this slope is maximum for the MPB compositions suggesting a greater degree of polar-heterogeneity at the MPB. ***d***, Rietveld fitted neutron powder diffraction patterns of two close by MPB compositions $x = 0.06$ and $x = 0.0675$ using $R3c$ + P4bm phase coexistence model. The misfit regions are highlighted in the insets and with arrow in the plot. The additional superlattice peak marked with arrow suggest the need for considering higher order modulation in the octahedral tilt configuration[93].

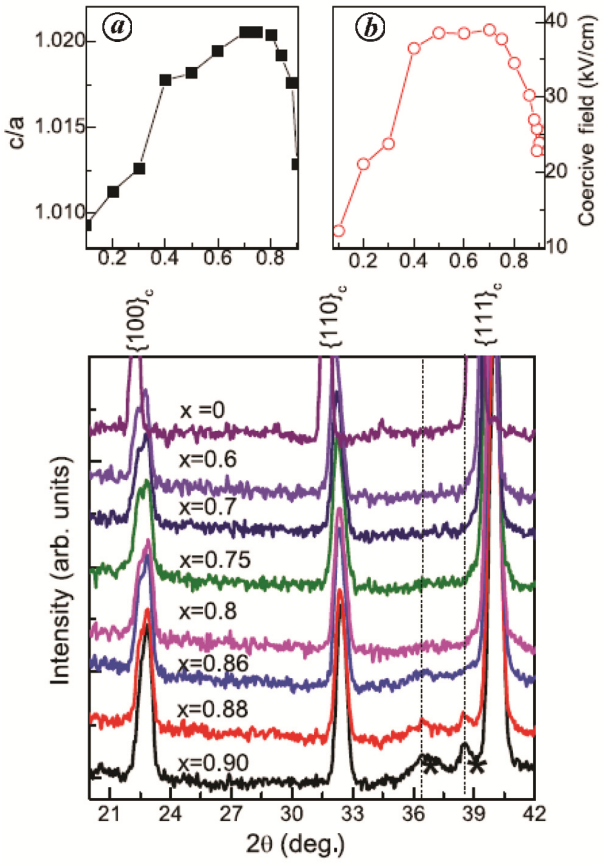

Figure 4. Composition dependence of (***a***) tetragonality and (***b***) coercive-field of $(1–x)BaTiO_3–(x)Na_{0.5}Bi_{0.5}TiO_3$. A maximum in both the quantities can be seen at $x = 0.80$. (***b***) The composition evolution of the neutron powder diffraction pattern of $(1–x)BaTiO_3–(x)Na_{0.5}Bi_{0.5}TiO_3$. The ½{310} superlattice peak corresponding to in-phase octahedral tilt appears for $x > 0.80$. The reduction in the tetragonality and coercive field for $x > 0.80$ is therefore attributed to the onset of the in-phase tilt[104].

others[37,38,137–143]. A glimpse of this behaviour is observed even in the unmodified NBT when heated above the depolarization temperature (200°C). At 400°C, NBT shows a unipolar electrostrain of ~0.4% at 80 kV/cm (ref. 142). The role of different modifications is to bring down the ergodic–non-ergodic relaxor transition temperature to just below room temperature. Strong electric field at room temperature can induce a ferroelectric state causing large electrostrain. The reproducibility of the large electrostrain in different cycles is possible because the system is capable of reverting back to its ergodic relaxor–ferroelectric state when the field is reduced to zero. In the situation, this does not happen completely, the electrostrain reduces in successive cycles[109]. The field induced ergodic–ferroelectric transitions are also interesting from the viewpoint of achieving enhanced electrocaloric response[141].

Factors influencing thermal depoling in NBT-based piezoelectrics

The mechanism governing thermal depoling/depolarization of NBT and its chemical derivatives is a subject of considerable debate. The absence of any anomaly in the elastic compliance of NBT at ~200°C led Cordero *et al.*[52] to suggest that the thermal depolarization is not driven by any kind of structural event. Aksel *et al.*[144] on the other hand, related the thermal depolarization at 200°C to structural transition on a smaller length scale. Rao *et al.*[45] have shown that the depoling process of NBT starts at ~150°C with the onset of in-phase octahedral tilt (Figure 5). For the two most investigated solid solutions, $(1–x)Na_{0.5}Bi_{0.5}TiO_3–xBaTiO_3$ (NBT–BT) and

$(1–y)Na_{0.5}Bi_{0.5}TiO_3–yK_{0.5}Bi_{0.5}TiO_3$ (NBT–KBT), exhibiting MPBs at $x = 0.06$ and $y = 0.20$ respectively, the depolarization temperature decreases sharply as the MPB is approached[87,116,132–134]. This scenario contrasts with other MPB ferroelectric systems where no such remarkable change in the Curie point is reported at the MPB[132–134] (Figure 6 *a–c*). Since the depolarization temperature is an indicator of the strength of the cooperative interaction of the neighbouring dipoles in a ferroelectric material, the anomalous dip in the depolarization temperature at the MPB of NBT–BT appears to indicate weakening of ferroelectricity at the MPB of NBT–BT. Recently Adhikary *et. al.*[132–134] have shown that as the MPB is approached, there is also an increasing intervention of a non-ferroelectric distortion in the form of in-phase tilt (Figure 6 *d* and *e*). The authors argue that the system's propensity for this non-ferroelectric distortion causes weakening of ferroelectricity leading to a dramatic decrease in the depolarization temperature at the MPB. The authors also suggested that this could be one of the reasons which limits the weak-signal electromechanical properties of NBT-based systems.

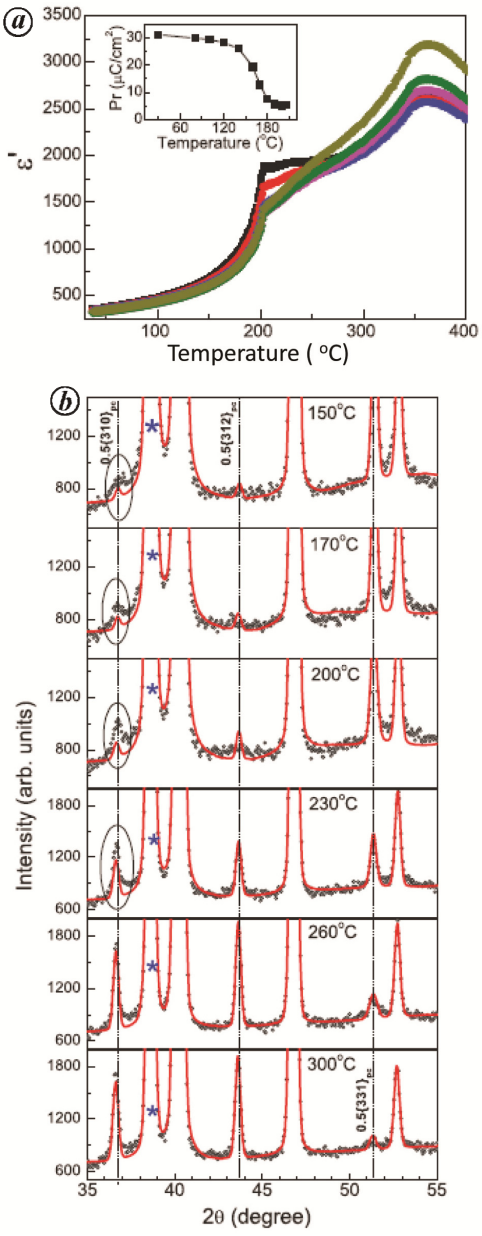

Figure 5. ***a***, The phenomenon of thermal depolarization in terms of an abrupt anomaly in the relative permittivity during heating of a poled NBT. The temperature dependence of remanent polarization (shown in the inset) starts to drop above 150°C. ***b***, The neutron powder diffraction of NBT collected at different temperatures (wavelength of neutron = 1.548183 Å). Important to note is the appearance of superlattice reflection of the ½{odd odd even} type such as 0.5{310} and 0.5{312} at 150°C. The intensity of these reflections increases fast above 200°C. These experiments confirm that the onset of thermal depolarization in NBT is due to appearance of in-phase tilted regions ~ 150°C. Being incompatible with ferroelectric distortion, these regions increasingly disturb the long-range ferroelectric order established in NBT by the poling field[45].

With increasing technological interest in NBT-based piezoelectrics in high power applications[17], attempts are also being made to improve their depolarization temperatures[145–150]. Zhang *et al.*[148] reported a composite approach to enhance the depolarization temperature without significantly compromising the piezoelectric properties. The authors demonstrated that dispersed ZnO grains amid the ferroelectric grains of the MPB composition $0.94Na_{0.5}Bi_{0.5}TiO_3–0.06BaTiO_3$ (NBT–6BT) led to increase in the depolarization temperature by ~40°C (i.e. from 90°C to 130°C). They hypothesized that the free charge carriers in the semiconducting ZnO grains screen the depolarizing field in the ferroelectric grains and sustain ferroelectricity up to a relatively higher temperature. Mahajan *et al.*[146] have questioned this electrostatic argument and argued in favour of a structural mechanism to explain thermal depolarization. Riemer *et al.*[149] argued that the sustenance of ferroelectricity up to higher temperature in the 0–3 NBT–6BT/ZnO composite is caused by deviatoric stress field due to difference in the thermal expansion coefficients of ZnO and the ferroelectric grains. A notable increase in the depolarization temperature has also been reported in non-composite specimens such as in Zn-doped NBT–6BT[150] thereby suggesting that the composite nature of the specimen need not be the primary factor influencing the delay in thermal depolarization of ZnO modified NBT-based piezoceramics. Recently Khatua *et al.*[107] demonstrated that the depolarization temperature of NBT-based piezoceramics is grain-size dependent (Figure 7). They established a coupled microstructural (grain size)–structural mechanism and show that the large grain-sized NBT specimens show higher depolarization temperature as compared to NBT with small grain size. Khatua *et al.*[107] demonstrated that the increase in the depolarization temperature in large grain size specimen is caused by larger grains able to stabilize large ferroelectric distortion after poling. The authors rationalized that instead of the screening-field stabilizing the ferroelectric phase in ZnO-doped NBT[107], it is the larger grain size of

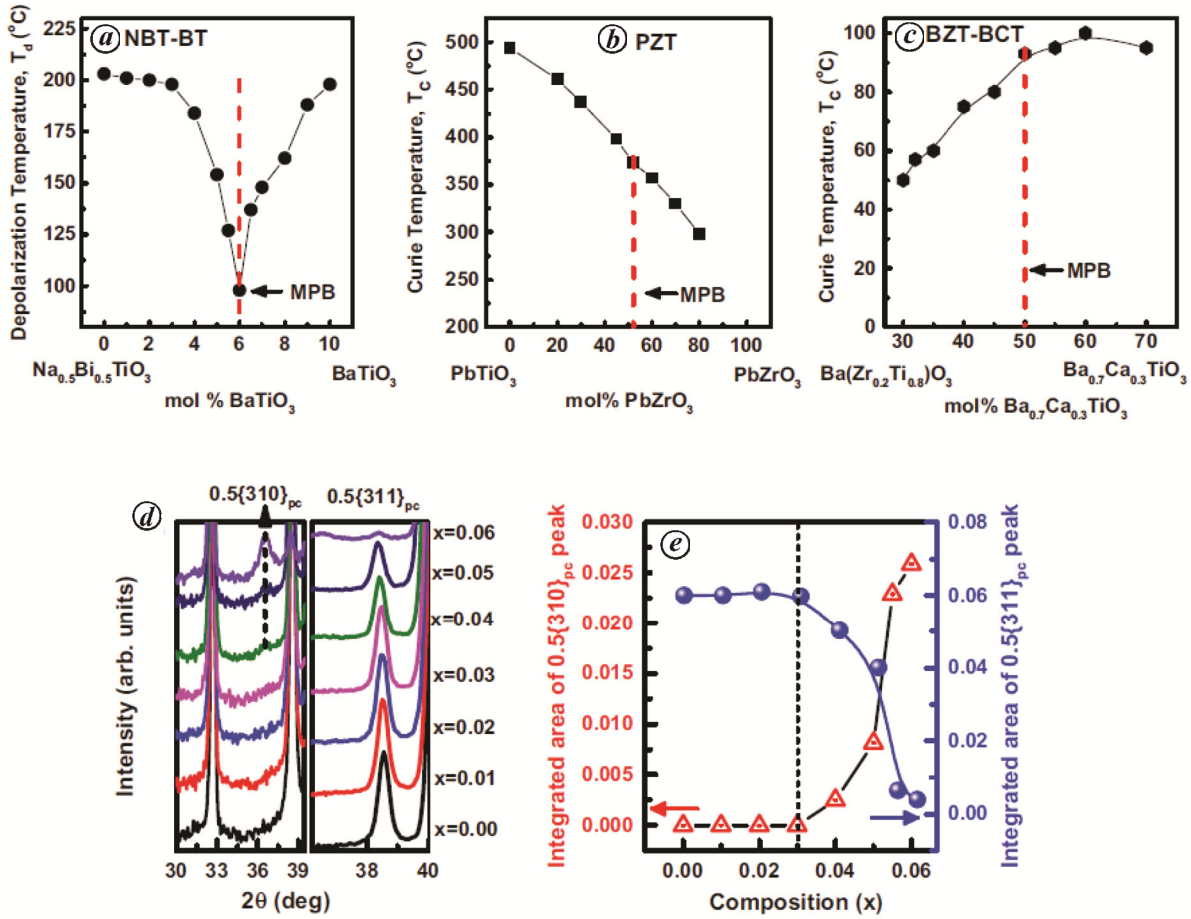

Figure 6. ***a–c***, Depolarization temperature/Curie point as a function of composition around the respective morphotropic phase boundaries of (***a***) $(1–x)Na_{0.5}Bi_{0.5}TiO_3–(x)BaTiO_3$, (***b***) $Pb(Zr_xTi_{1-x})O_3$ and (***c***) $(1–x)BaZr_{0.8}Ti_{0.8}O_3–(x)Ba_{0.7}Ca_{0.3}TiO_3$ piezoelectric systems. Note the anomalous dip at the MPB in the NBT–BT and not so in the other two systems. ***d***, The composition dependence of evolution of the 0.5{310} and 0.5{311} superlattice peaks as observed in the neutron powder diffraction of the specimens. ***e***, The peak intensity of these two superlattice peaks plotted on a normalized scale (treating the background corrected peak count of the strongest reflection as 100). Note the significant increase in the intensity of the 0.5{310} superlattice peak corresponding to in-phase octahedral tilt at the MPB ($x = 0.06$). A concomitant decrease in the intensity of the 0.5{311} superlattice peak, corresponding to the *R*3*c* phase is also evident at the MPB composition[134].

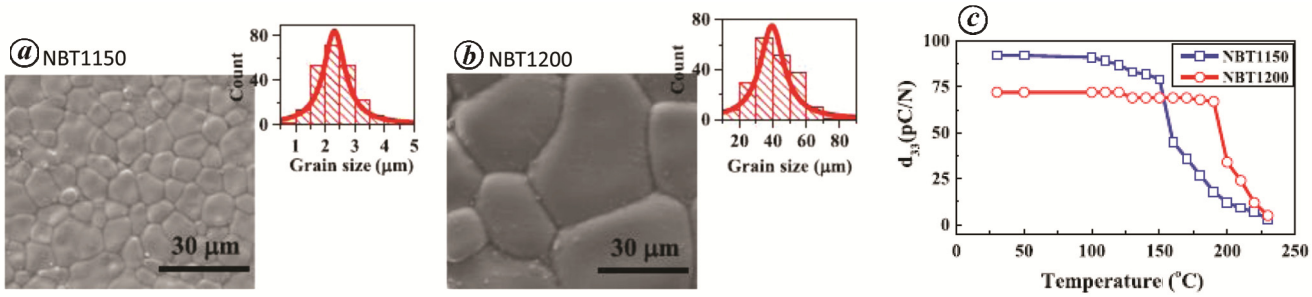

Figure 7. Scanning electron microscope images (secondary electron image) of NBT sintered at (***a***) 1150°C and (***b***) 1200°C. (***c***) Thermal depoling of the two specimens by measuring d_{33} as a function of the thermal aging temperature. Note the higher depolarization temperature of the NBT1200 with significantly larger grain size[107].

the ZnO-modified specimens and the corresponding stabilization of the relatively large ferroelectric distortion after poling in such specimens which causes the increase in the depolarization temperature.

Summary and outlook

Regulations on the restricted use of hazardous materials in several countries across the world have given a great

thrust to research and development in Pb-free piezoceramics. While some lead-free compositions have found applications in niche products, a PZT like universal lead-free piezoelectric material system for wide ranging applications is still not on the horizon. This urgency has however helped in discovering new Pb-free systems with large electromechanical properties, and helped in developing deeper scientific understanding of some of the complex issues related to structure–property correlations. Regarding NBT-based piezoceramics, it is now evident that a highly complex inter-relationship exists between synthesis conditions, grain size, length scale dependent crystal structures and physical properties. As highlighted in this review, an important structural feature associated with structural–polar disorder is the system's propensity for stabilizing in-phase octahedral tilt which is incompatible with ferroelectric order. Recent research shows that this propensity is maximum at the MPB of NBT–BT and NBT–KBT systems. The consequent weakening of the strength of ferroelectric interaction causes lowering of the depolarization temperature and, perhaps, also not allowing the system to develop large piezoelectric response (comparable to what has been achieved in other Pb-free piezoelectrics). It is anticipated that large piezoelectric response in NBT-based piezoelectrics requires strategies which can suppress the system propensity for this in-phase octahedral tilt. At the same time, this tilt disorder appears to be playing an important role in enabling the system to exhibit large high-field electrostrain making them interesting for high performance actuator applications.

1. Curie, J. and Curie, P., Development by pressure of polar electricity in hemihedral crystals with inclined faces. *Bull. Soc. Min. de France*, 1880, **3**, 90.
2. Uchino, K., *Ferroelectric Devices*, Marcel Dekker, New York, 2000.
3. Nye, J. F., *Physical Properties of Crystals: their Representation by Tensors and Matrices*, Oxford University Press, 1985.
4. Newnham, R. E., *Properties of Materials: Anisotropy, Symmetry, Structure*. Oxford University Press on Demand, 2005.
5. Busch, G., Early history of ferroelectricity. *Ferroelectrics*, 1987, **74**, 267–284.
6. Jaffe, B., Cook, W. R. and Jaffe, H., *Piezoelectric Ceramics*, Academic Press, 1971, pp. 135–183.
7. Haertling, G. H., Ferroelectric ceramics: history and technology. *J. Am. Ceram. Soc.,* 1999, **82**, 797–818.
8. Damjanovic, D., Contributions to the piezoelectric effect in ferroelectric single crystals and ceramics. *J. Am. Ceram. Soc*., 2005, **88**, 2663–2676.
9. Damjanovic, D., Ferroelectric, dielectric and piezoelectric properties of ferroelectric thin films and ceramics. *Rep. Prog. Phys*., 1998, **61**, 1267.
10. Jin, Y. M., Wang, Y. U., Khachaturyan, A. G., Li, J. F. and Viehland, D., Conformal miniaturization of domains with low domain-wall energy: Monoclinic ferroelectric states near the morphotropic phase boundaries. *Phys. Rev. Lett*., 2003, **91**, 97601.
11. Directive, E. U., Restriction of the use of certain hazardous substances in electrical and electronic equipment (RoHS). *Off. J. Eur. Commun*., 2013, **46**, 19–23.
12. Maeder, M. D., Damjanovic, D. and Setter, N., Lead free piezoelectric materials. *J. Electroceram*., 2004, **13**, 385–392.
13. Rödel, J., Jo, W., Seifert, K. T., Anton, E. M., Granzow, T. and Damjanovic, D., Perspective on the development of lead-free piezoceramics. *J. Am. Ceram. Soc.*, 2009, **92**, 1153–1177.
14. Panda, P. K., Environmental friendly lead-free piezoelectric materials. *J. Mater. Sci*., 2009, **44**, 5049–5062.
15. Rödel, J., Webber, K. G., Dittmer, R., Jo, W., Kimura, M. and Damjanovic, D., Transferring lead-free piezoelectric ceramics into application. *J. Eur. Ceram. Soc.*, 2015, **35**, 1659–1681.
16. Zheng, T., Wu, J., Xiao, D. and Zhu, J., Recent development in lead-free perovskite piezoelectric bulk materials. *Prog. Mater. Sci.*, 2018, **98**, 552–624.
17. Shibata, K., Wang, R., Tou, T. and Koruza, J., Applications of lead-free piezoelectric materials. *MRS Bull.*, 2018, **43**, 612–616.
18. Wang, K., Malič, B. and Wu, J., Shifting the phase boundary: Potassium sodium niobate derivates. *MRS Bull.*, 2018, **43**, 607–611.
19. Gao, J., Ke, X., Acosta, M., Glaum, J. and Ren, X., High piezoelectricity by multiphase coexisting point: Barium titanate derivatives. *MRS Bull.*, 2018, **43**, 595–599.
20. Paterson, A. R. *et al.*, Relaxor-ferroelectric transitions: Sodium bismuth titanate derivatives. *MRS Bull.*, 2018, **43**, 600–606.
21. Reichmann, K., Feteira, A. and Li, M., Bismuth sodium titanate based materials for piezoelectric actuators. *Materials*, 2015, **8**, 8467–8495.
22. Saito, Y. *et al.*, Lead-free piezoceramics. *Nature*, 2004, **432**, 84.
23. Xu, K., Li, J., Lv, X., Wu, J., Zhang, X., Xiao, D. and Zhu, J., Superior piezoelectric properties in potassium–sodium niobate lead-free ceramics. *Adv. Mater.*, 2016, **28**, 8519–8523.
24. Brajesh, K., Kalyani, A. K. and Ranjan, R., Ferroelectric instabilities and enhanced piezoelectric response in Ce modified $BaTiO_3$ lead-free ceramics. *Appl. Phys. Lett.*, 2015, **106**, 012907.
25. Kalyani, A. K., Krishnan, H., Sen, A., Senyshyn, A. and Ranjan, R., Polarization switching and high piezoelectric response in Sn-modified $BaTiO_3$. *Phys. Rev. B.*, 2015, **91**, 024101.
26. Kalyani, A. K., Brajesh, K., Senyshyn, A. and Ranjan, R., Orthorhombic-tetragonal phase coexistence and enhanced piezoresponse at room temperature in Zr, Sn, and Hf modified $BaTiO_3$. *Appl. Phys. Lett.*, 2014, **104**, 252906.
27. Brajesh, K., Tanwar, K., Abebe, M. and Ranjan, R., Relaxor ferroelectricity and electric-field-driven structural transformation in the giant lead-free piezoelectric $(Ba,Ca)(Ti,Zr)O_3$. *Phys. Rev. B.*, 2015, **92**, 224112.
28. Liu, W. and Ren, X., Large piezoelectric effect in Pb-free ceramics. *Phys. Rev. Lett.*, 2009, **103**, 257602.
29. Acosta, M. *et al.*, Piezoelectricity and rotostriction through polar and non-polar coupled instabilities in bismuth-based piezoceramics. *Sci. Rep.*, 2016, **6**, 28742.
30. Abebe, M., Brajesh, K., Mishra, A., Senyshyn, A. and Ranjan, R., Structural perspective on the anomalous weak-field piezoelectric response at the polymorphic phase boundaries of $(Ba,Ca)(Ti,M)O_3$ lead-free piezoelectrics (M = Zr, Sn, Hf). *Phys. Rev. B.*, 2017, **96**, 014113.
31. Xue, D., Zhou, Y., Bao, H., Gao, J., Zhou, C. and Ren, X., Large piezoelectric effect in Pb-free $Ba(Ti,Sn)O_3$–$x(Ba,Ca)TiO_3$ ceramics. *Appl. Phys. Lett*., 2011, **99**, 122901.
32. Zhou, C., Liu, W., Xue, D., Ren, X., Bao, H., Gao, J. and Zhang, L., Triple-point-type morphotropic phase boundary based large piezoelectric Pb-free material – $Ba(Ti_{0.8}Hf_{0.2})O_3$–$(Ba_{0.7}Ca_{0.3})$–TiO_3. *Appl. Phys. Lett.*, 2012, **100**, 222910.
33. Catalan, G. and Scott, J. F., Physics and applications of bismuth ferrite. *Adv. Mater.*, 2009, **21**, 2463–2485.
34. Lee, M. H. *et al.*, High-performance lead-free piezoceramics with high curie temperatures. *Adv. Mater.*, 2015, **2743**, 6976–6982.

35. Yang, S. C., Kumar, A., Petkov, V. and Priya, S., Room-temperature magnetoelectric coupling in single-phase $BaTiO_3$–$BiFeO_3$ system. *J. Appl. Phys.*, 2013, **113**, 144101.
36. Yang, H., Zhou, C., Liu, X., Zhou, Q., Chen, G., Li, W. and Wang, H., Piezoelectric properties and temperature stabilities of Mn- and Cu-modified $BiFeO_3$–$BaTiO_3$ high temperature ceramics. *J. Eur. Ceram. Soc.*, 2013, **33**, 1177–1183.
37. Liu, X. and Tan, X., Giant strain with low cycling degradation in Ta-doped $[Bi_{1/2}(Na_{0.8}K_{0.2})_{1/2}]TiO_3$ lead-free ceramics. *J. Appl. Phys.*, 2016, **120**, 034102.
38. Li, T. *et al.*, Giant strain with low hysteresis in A-site-deficient $(Bi_{0.5}Na_{0.5})TiO_3$-based lead-free piezoceramics. *Acta Mater.*, 2017, **128**, 337–344.
39. Smolensky, G. A., Isupov, V. A., Agranovskaya, A. I. and Krainik, N. N., New materials of AIIBIVOVI type. *Trans. Sov. Phys. Solid State*, 1961, **2**, 2651–2654.
40. Pronin, I. P., Syrnikov, P. P., Isupov, V. A., Egorov, V. M. and Zaitseva, N. V., Peculiarities of phase transitions in sodium-bismuth titanate. *Ferroelectrics*, 1980, **25**, 395–397.
41. Sakata, K. and Masuda, Y., Ferroelectric and antiferroelectric properties of $(Na_{0.5}Bi_{0.5})TiO_3$–$SrTiO_3$ solid solution ceramics. *Ferroelectrics*, 1974, **7**, 347–349.
42. Isupov, V. A., Ferroelectric $Na_{0.5}Bi_{0.5}TiO_3$ and $K_{0.5}Bi_{0.5}TiO_3$ perovskites and their solid solutions. *Ferroelectrics*, 2005, **315**, 123–147.
43. Suchanicz, J., Investigations of the phase transitions in $Na_{0.5}Bi_{0.5}TiO_3$. *Ferroelectrics*, 1995, **172**, 455–458.
44. Tu, C. S., Siny, I. G. and Schmidt, V. H., Sequence of dielectric anomalies and high-temperature relaxation behavior in $Na_{1/2}Bi_{1/2}TiO_3$. *Phys. Rev. B.*, 1994, **49**, 11550.
45. Rao, B. N., Datta, R., Chandrashekaran, S. S., Mishra, D. K., Sathe, V., Senyshyn, A. and Ranjan, R., Local structural disorder and its influence on the average global structure and polar properties in $Na_{0.5}Bi_{0.5}TiO_3$. *Phys. Rev. B.*, 2013, **88**, 224103.
46. Petzelt, J. *et al.*, Infrared, Raman and high-frequency dielectric spectroscopy and the phase transitions in $Na_{1/2}Bi_{1/2}TiO_3$. *J. Phys.: Condens. Matter*, 2004, **16**, 2719.
47. Gorfman, S., Glazer, A. M., Noguchi, Y., Miyayama, M., Luo, H. and Thomas, P. A., Observation of a low-symmetry phase in $Na_{0.5}Bi_{0.5}TiO_3$ crystals by optical birefringence microscopy. *J. Appl. Crystallogr.*, 2012, **45**, 444–452.
48. Suchanicz, J., Roleder, K., Kania, A. and Hańaderek, J., Electrostrictive strain and pyroeffect in the region of phase coexistence in $Na_{0.5}Bi_{0.5}TiO_3$. *Ferroelectrics*, 1988, **77**, 107–110.
49. Vakhrushev, S. B., Isupov, V. A., Kvyatkovsky, B. E., Okuneva, N. M., Pronin, I. P., Smolensky, G. A. and Syrnikov, P. P., Phase transitions and soft modes in sodium bismuth titanate. *Ferroelectrics*, 1985, **63**, 153–160.
50. Siny, I. G., Smirnova, T. A. and Kruzina, T. V., The phase transition dynamics in $Na_{1/2}Bi_{1/2}TiO_3$. *Ferroelectrics*, 1991, **124**, 207–212.
51. Jones, G. O. and Thomas, P. A., Investigation of the structure and phase transitions in the novel A-site substituted distorted perovskite compound $Na_{0.5}Bi_{0.5}TiO_3$. *Acta Crystallogr. B.*, 2002, **58**, 168–178.
52. Cordero, F., Craciun, F., Trequattrini, F., Mercadelli, E. and Galassi, C., Phase transitions and phase diagram of the ferroelectric perovskite $(Na_{0.5}Bi_{0.5})_{1-x}Ba_xTiO_3$ by anelastic and dielectric measurements. *Phys. Rev. B.*, 2010, **81**, 144124.
53. Dorcet, V., Trolliard, G. and Boullay, P., Reinvestigation of phase transitions in $Na_{0.5}Bi_{0.5}TiO_3$ by TEM. Part I: First order rhombohedral to orthorhombic phase transition. *Chem. Mater.*, 2008, **20**, 5061–5073.
54. Trolliard, G. and Dorcet, V., Reinvestigation of phase transitions in $Na_{0.5}Bi_{0.5}TiO_3$ by TEM. Part II: Second order orthorhombic to tetragonal phase transition. *Chem. Mater.*, 2008, **20**, 5074–5082.
55. Balagurov, A. M., Koroleva, E. Y., Naberezhnov, A. A., Sakhnenko, V. P., Savenko, B. N., Ter-Oganessian, N. V. and Vakhrushev, S. B., The rhombohedral phase with incommensurate modulation in $Na_{1/2}Bi_{1/2}TiO_3$. *Phase Transit.*, 2006, **79**, 163–173.
56. Thomas, P. A., Trujillo, S., Boudard, M., Gorfman, S. and Kreisel, J., Diffuse X-ray scattering in the lead-free piezoelectric crystals $Na_{1/2}Bi_{1/2}TiO_3$ and Ba-doped $Na_{1/2}Bi_{1/2}TiO_3$. *Solid State Sci.*, 2010, **12**, 311–317.
57. Kreisel, J. *et al.*, High-pressure X-ray scattering of oxides with a nanoscale local structure: Application to $Na_{1/2}Bi_{1/2}TiO_3$. *Phys. Rev. B.*, 2003, **68**, 014113.
58. Keeble, D. S., Barney, E. R., Keen, D. A., Tucker, M. G., Kreisel, J. and Thomas, P. A., Bifurcated polarization rotation in bismuth-based piezoelectrics. *Adv. Funct. Mater.*, 2013, **23**, 185–190.
59. Groeting, M., Hayn, S. and Albe, K., Chemical order and local structure of the lead-free relaxor ferroelectric $Na_{1/2}Bi_{1/2}TiO_3$. *J. Solid State Chem.*, 2011, **184**, 2041–2046.
60. Gröting, M., Kornev, I., Dkhil, B. and Albe, K., Pressure-induced phase transitions and structure of chemically ordered nanoregions in the lead-free relaxor ferroelectric $Na_{1/2}Bi_{1/2}TiO_3$. *Phys. Rev. B.*, 2012, **86**, 134118.
61. Groszewicz, P. B., Gröting, M., Breitzke, H., Jo, W., Albe, K., Buntkowsky, G. and Rödel, J., Reconciling local structure disorder and the relaxor state in $(Bi_{1/2}Na_{1/2})TiO_3$–$BaTiO_3$. *Sci. Rep.*, 2016, **6**, 31739.
62. Shuvaeva, V. A., Zekria, D., Glazer, A. M., Jiang, Q., Weber, S. M., Bhattacharya, P. and Thomas, P. A., Local structure of the lead-free relaxor ferroelectric $(K_xNa_{1-x})_{0.5}Bi_{0.5}TiO_3$. *Phys. Rev. B.*, 2005, **71**, 174114.
63. Rao, B. N., Olivi, L., Sathe, V. and Ranjan, R., Electric field and temperature dependence of the local structural disorder in the lead-free ferroelectric $Na_{0.5}Bi_{0.5}TiO_3$: an EXAFS study. *Phys. Rev. B.*, 2016, **93**, 024106.
64. Aksel, E., Forrester, J. S., Nino, J. C., Page, K., Shoemaker, D. P. and Jones, J. L., Local atomic structure deviation from average structure of $Na_{0.5}Bi_{0.5}TiO_3$: combined X-ray and neutron total scattering study. *Phys. Rev. B.*, 2013, **87**, 104113.
65. Groszewicz, P. B., Breitzke, H., Dittmer, R., Sapper, E., Jo, W., Buntkowsky, G. and Rödel, J., Nanoscale phase quantification in lead-free $(Bi_{1/2}Na_{1/2})TiO_3$–$BaTiO_3$ relaxor ferroelectrics by means of Na 23 NMR. *Phys. Rev. B.*, 2014, **90**, 220104.
66. Groszewicz, P. B., Breitzke, H., Jo, W., Rödel, J. and Buntkowsky, G., Local Structure of the B-site in BNT-*x*BT Investigated by 47, 49Ti NMR: Effect of barium content. *J. Appl. Phys.*, 2017, **121**, 114104.
67. Gorfman, S. and Thomas, P. A., Evidence for a non-rhombohedral average structure in the lead-free piezoelectric material $Na_{0.5}Bi_{0.5}TiO_3$. *J. Appl. Crystallogr.*, 2010, **43**, 1409–1414.
68. Aksel, E., Forrester, J. S., Jones, J. L., Thomas, P. A., Page, K. and Suchomel, M. R., Monoclinic crystal structure of polycrystalline $Na_{0.5}Bi_{0.5}TiO_3$. *Appl. Phys. Lett.*, 2011, **98**, 152901.
69. Levin, I. and Reaney, I. M., Nano- and mesoscale structure of $Na_{1/2}Bi_{1/2}TiO_3$: a TEM perspective. *Adv. Funct. Mater.*, 2012, **22**, 3445–3452.
70. Rao, B. N., Fitch, A. N. and Ranjan, R., Ferroelectric-ferroelectric phase coexistence in $Na_{1/2}Bi_{1/2}TiO_3$. *Phys. Rev. B.*, 2013, **87**, 060102.
71. Rao, B. N. and Ranjan, R., Electric-field-driven monoclinic-to-rhombohedral transformation in $Na_{1/2}Bi_{1/2}TiO_3$. *Phys. Rev. B.*, 2012, **86**, 134103.
72. Beanland, R. and Thomas, P. A., Symmetry and defects in rhombohedral single-crystalline $Na_{0.5}Bi_{0.5}TiO_3$. *Phys. Rev. B.*, 2014, **89**, 174102.

73. Usher, T. M., Levin, I., Daniels, J. E. and Jones, J. L., Electric-field-induced local and mesoscale structural changes in polycrystalline dielectrics and ferroelectrics. *Sci. Rep.*, 2015, **5**, 14678.
74. Khatua, D. K., Mehrotra, T., Mishra, A., Majumdar, B., Senyshyn, A. and Ranjan, R., Anomalous influence of grain size on the global structure, ferroelectric and piezoelectric response of $Na_{0.5}Bi_{0.5}TiO_3$. *Acta Mater.*, 2017, **134**, 177–187.
75. Mishra, A., Khatua, D. K., De, A., Majumdar, B., Frömling, T. and Ranjan, R., Structural mechanism behind piezoelectric enhancement in off-stoichiometric $Na_{0.5}Bi_{0.5}TiO_3$ based lead-free piezoceramics. *Acta Mater.*, 2019, **164**, 761–775.
76. Park, S. E., Chung, S. J., Kim, I. T. and Hong, K. S., Nonstoichiometry and the long-range cation ordering in crystals of $(Na_{1/2}Bi_{1/2})TiO_3$. *J. Am. Ceram. Soc.*, 1994, **77**, 2641–2647.
77. Zuo, R., Su, S., Wu, Y., Fu, J., Wang, M. and Li, L., Influence of A-site nonstoichiometry on sintering, microstructure and electrical properties of $(Bi_{0.5}Na_{0.5})TiO_3$ ceramics. *Mater. Chem. Phys.*, 2008, **110**, 311–315.
78. Sung, Y. S. *et al.*, Effects of Na nonstoichiometry in $(Bi_{0.5}Na_{0.5+x})TiO_3$ ceramics. *Appl. Phys. Lett.*, 2010, **96**, 022901.
79. Sung, Y. S., Kim, J. M., Cho, J. H., Song, T. K., Kim, M. H. and Park, T. G., Effects of Bi nonstoichiometry in $(Bi_{0.5+x}Na_{0.5})TiO_3$ ceramics. *Appl. Phys. Lett.*, 2011, **98**, 012902.
80. Carter, J., Aksel, E., Iamsasri, T., Forrester, J. S., Chen, J. and Jones, J. L., Structure and ferroelectricity of nonstoichiometric $(Na_{0.5}Bi_{0.5})TiO_3$. *Appl. Phys. Lett.*, 2014, **104**, 112904.
81. Spreitzer, M., Valant, M. and Suvorov, D., Sodium deficiency in $Na_{0.5}Bi_{0.5}TiO_3$. *J. Mater. Chem.*, 2007, **17**, 185–192.
82. Naderer, M., Kainz, T., Schütz, D. and Reichmann, K., The influence of Ti-nonstoichiometry in $Bi_{0.5}Na_{0.5}TiO_3$. *J. Eur. Ceram. Soc.*, 2014, **34**, 663–667.
83. Mishra, A., Khatua, D. K., Adhikary, G. D., Kumar, N., Shankar, U. and Ranjan, R., Finite-size-effect on a very large length scale in NBT-based lead-free piezoelectrics. *J. Adv. Dielectr.*, 2019, **9**, 1950035.
84. Mishra, A., Khatua, D. K., De, A. and Ranjan, R., Off-stoichiometry, structural-polar disorder and piezoelectricity enhancement in pre-MPB lead-free $Na_{0.5}Bi_{0.5}TiO_3$–$BaTiO_3$ piezoceramic. *J. Appl. Phys.*, 2019, **125**, 214101.
85. Li, M., Zhang, H., Cook, S. N., Li, L., Kilner, J. A., Reaney, I. M. and Sinclair, D. C., Dramatic influence of A-site nonstoichiometry on the electrical conductivity and conduction mechanisms in the perovskite oxide $Na_{0.5}Bi_{0.5}TiO_3$. *Chem. Mater.*, 2015, **27**, 629–634.
86. Takenaka, T., Maruyama, K. I. and Sakata, K., $(Bi_{1/2}Na_{1/2})TiO_3$–$BaTiO_3$ system for lead-free piezoelectric ceramics. *Jpn. J. Appl. Phys.*, 1991, **30**, 2236.
87. Ranjan, R. and Dviwedi, A., Structure and dielectric properties of $(Na_{0.50}Bi_{0.50})_{1-x}Ba_xTiO_3$: $0 \le x \le 0.10$. *Solid State Commun.*, 2005, **135**, 394–399.
88. Jo, W., Daniels, J. E., Jones, J. L., Tan, X., Thomas, P. A., Damjanovic, D. and Rödel, J., Evolving morphotropic phase boundary in lead-free $(Bi_{1/2}Na_{1/2})TiO_3$–$BaTiO_3$ piezoceramics. *J. Appl. Phys.*, 2011, **109**, 014110.
89. Wylie-van Eerd, B., Damjanovic, D., Klein, N., Setter, N. and Trodahl, J., Structural complexity of $(Na_{0.5}Bi_{0.5})TiO_3$–$BaTiO_3$ as revealed by Raman spectroscopy. *Phys. Rev. B.*, 2010, **82**, 104112.
90. Ma, C., Tan, X., Dul'Kin, E. and Roth, M., Domain structure-dielectric property relationship in lead-free $(1–x)(Bi_{1/2}Na_{1/2})$–TiO_3–$x$$BaTiO_3$ ceramics. *J. Appl. Phys.*, 2010, **108**, 104105.
91. Garg, R., Rao, B. N., Senyshyn, A., Krishna, P. S. R. and Ranjan, R., Lead-free piezoelectric system $(Na_{0.5}Bi_{0.5})TiO_3$–$BaTiO_3$: Equilibrium structures and irreversible structural transformations driven by electric field and mechanical impact. *Phys. Rev. B.*, 2013, **88**, 014103.
92. Daniels, J. E., Jo, W., Rödel, J., Rytz, D. and Donner, W., Structural origins of relaxor behavior in a 0.96 $(Bi_{1/2}Na_{1/2})TiO_3$–$0.04BaTiO_3$ single crystal under electric field. *Appl. Phys. Lett.*, 2011, **98**, 252904.
93. Garg, R., Narayana Rao, B., Senyshyn, A. and Ranjan, R., Long ranged structural modulation in the pre-morphotropic phase boundary cubic-like state of the lead-free piezoelectric $Na_{1/2}Bi_{1/2}TiO_3$–$BaTiO_3$. *J. Appl. Phys.*, 2013, **114**, 234102.
94. Datta, K., Neder, R. B., Richter, A., Göbbels, M., Neuefeind, J. C. and Mihailova, B., Adaptive strain prompting a pseudo-morphotropic phase boundary in ferroelectric $(1–x)Na_{0.5}Bi_{0.5}$-TiO_3–$x$$BaTiO_3$. *Phys. Rev. B.*, 2018, **97**, 184101.
95. Datta, K., Richter, A., Göbbels, M., Neder, R. B. and Mihailova, B., Atomistic origin of huge response functions at the morphotropic phase boundary of $(1–x)Na_{0.5}Bi_{0.5}TiO_3$–$x$$BaTiO_3$. *Phys. Rev. B.*, 2014, **90**, 064112.
96. Yao, J. *et al.*, Evolution of domain structures in $Na_{1/2}Bi_{1/2}TiO_3$ single crystals with $BaTiO_3$. *Phys. Rev. B.*, 2011, **83**, 054107.
97. Chen, M., Xu, Q., Kim, B. H., Ahn, B. K., Ko, J. H., Kang, W. J. and Nam, O. J., Structure and electrical properties of $(Na_{0.5}Bi_{0.5})_{1-x}Ba_xTiO_3$ piezoelectric ceramics. *J. Eur. Ceramic Soc.*, 2008, **28**, 843–849.
98. Daniels, J. E., Jo, W., Rödel, J. and Jones, J. L., Electric-field-induced phase transformation at a lead-free morphotropic phase boundary: Case study in a 93% $(Bi_{0.5}Na_{0.5})TiO_3$–7%$BaTiO_3$ piezoelectric ceramic. *Appl. Phys. Lett.*, 2009, **95**, 032904.
99. Ge, W., Cao, H., Li, J., Viehland, D., Zhang, Q. and Luo, H., Influence of dc-bias on phase stability in Mn-doped $Na_{0.5}Bi_{0.5}TiO_3$–5.6 at% $BaTiO_3$ single crystals. *Appl. Phys. Lett.*, 2009, **95**, 162903.
100. Chiang, Y. M., Farrey, G. W. and Soukhojak, A. N., Lead-free high-strain single-crystal piezoelectrics in the alkaline–bismuth–titanate perovskite family. *Appl. Phys. Lett.*, 1998, **73**, 3683–3685.
101. Ma, C., Guo, H. and Tan, X., A new phase boundary in $(Bi_{1/2}Na_{1/2})TiO_3$–$BaTiO_3$ revealed via a novel method of electron diffraction analysis. *Adv. Funct. Mater.*, 2013, **23**, 5261–5266.
102. Tan, X., Ma, C., Frederick, J., Beckman, S. and Webber, K. G., The antiferroelectric ↔ ferroelectric phase transition in lead-containing and lead-free perovskite ceramics. *J. Am. Ceram. Soc.*, 2011, **94**, 4091–4107.
103. Ma, C., Guo, H., Beckman, S. P. and Tan, X., Creation and destruction of morphotropic phase boundaries through electrical poling: a case study of lead-free $(Bi_{1/2}Na_{1/2})TiO_3$–$BaTiO_3$ piezoelectrics. *Phys. Rev. Lett.*, 2012, **109**, 107602.
104. Rao, B. N., Avdeev, M., Kennedy, B. and Ranjan, R., Phase boundary at $x = 0.03$ and its anomalous influence on the structure and properties in the lead-free piezoelectric $(1–x)Na_{1/2}Bi_{1/2}TiO_3$–$(x)BaTiO_3$. *Phys. Rev. B.*, 2015, **92**, 214107.
105. Rao, B. N., Khatua, D. K., Garg, R., Senyshyn, A. and Ranjan, R., Structural crossover from nonmodulated to long-period modulated tetragonal phase and anomalous change in ferroelectric properties in the lead-free piezoelectric $Na_{1/2}Bi_{1/2}TiO_3$–$BaTiO_3$. *Phys. Rev. B.*, 2015, **91**, 214116.
106. Maurya, D., Pramanick, A., Feygenson, M., Neuefeind, J. C., Bodnar, R. J. and Priya, S., Effect of poling on nanodomains and nanoscale structure in A-site disordered lead-free piezoelectric $Na_{0.5}Bi_{0.5}TiO_3$–$BaTiO_3$. *J. Mater. Chem. C.*, 2014, **2**, 8423–8431.
107. Khatua, D. K., Mishra, A., Kumar, N., Adhikary, G. D., Shankar, U., Majumdar, B. and Ranjan, R., A coupled microstructural-structural mechanism governing thermal depolarization delay in $Na_{0.5}Bi_{0.5}TiO_3$-based piezoelectrics. *Acta Mater.*, 2019, **179**, 49–60.
108. Khatua, D. K., Agarwal, A., Kumar, N. and Ranjan, R., Probing local structure of the morphotropic phase boundary composition of $Na_{0.5}Bi_{0.5}TiO_3$–$BaTiO_3$ using rare-earth photoluminescence as a technique. *Acta Mater.*, 2018, **145**, 429–436.

109. Khatua, D. K., Senyshyn, A. and Ranjan, R., Long-period modulated structure and electric-field-induced structural transformation in $Na_{0.5}Bi_{0.5}TiO_3$-based lead-free piezoelectrics. *Phys. Rev. B.*, 2016, **93**, 134106.
110. Khatua, D. K., Kalaskar, A. and Ranjan, R., Tuning photoluminescence response by electric field in electrically soft ferroelectrics. *Phys. Rev. Lett.*, 2016, **116**, 117601.
111. Jo, W., Daniels, J., Damjanovic, D., Kleemann, W. and Rödel, J., Two-stage processes of electrically induced-ferroelectric to relaxor transition in $0.94(Bi_{1/2}Na_{1/2})TiO_3$–$0.06BaTiO_3$. *Appl. Phys. Lett.*, 2013, **102**, 192903.
112. Anthoniappen, J. *et al.*, Enhanced piezoelectric and dielectric responses in 92.5% $(Bi_{0.5}Na_{0.5})TiO_3$−7.5% $BaTiO_3$ ceramics. *J. Am. Ceram. Soc.*, 2014, **97**, 1890–1894.
113. Parija, B., Badapanda, T., Panigrahi, S. and Sinha, T. P., Ferroelectric and piezoelectric properties of $(1–x)(Bi_{0.5}Na_{0.5})TiO_3$–$x BaTiO_3$ ceramics. *J. Mater. Sci.: Mater. Electron.*, 2013, **24**, 402–410.
114. Pronin, I. P., Parfenova, N. N., Zaitseva, N. V., Isupov, V. A. and Smolenskii, G. A., Phase transitions in solid solutions of sodiumbismuth and potassiumbismuth titanates. *Sov. Phys. Solid State.*, 1982, **24**, 1060–1062.
115. Sasaki, A., Chiba, T., Mamiya, Y. and Otsuki, E., Dielectric and piezoelectric properties of $(Bi_{0.5}Na_{0.5})TiO_3$–$(Bi_{0.5}K_{0.5})TiO_3$ systems. *Jpn. J. Appl. Phys.*, 1999, **38**, 5564.
116. Otoničar, M., Škapin, S. D., Spreitzer, M. and Suvorov, D., Compositional range and electrical properties of the morphotropic phase boundary in the $Na_{0.5}Bi_{0.5}TiO_3$–$K_{0.5}Bi_{0.5}TiO_3$ system. *J. Eur. Ceram. Soc.*, 2010, **30**, 971–979.
117. Jones, G. O., Kreisel, J. and Thomas, P. A., A structural study of the $(Na_{1–x}K_x)_{0.5}Bi_{0.5}TiO_3$ perovskite series as a function of substitution (x) and temperature. *Powder Diffr.*, 2002, **17**, 301–319.
118. Roleder, K., Franke, I., Glazer, A. M., Thomas, P. A., Miga, S. and Suchanicz, J., The piezoelectric effect in $Na_{0.5}Bi_{0.5}TiO_3$ ceramics. *J. Phys.: Condens. Matter.*, 2002, **14**, 5399.
119. Levin, I. *et al.*, Local structure, pseudosymmetry, and phase transitions in $Na_{1/2}Bi_{1/2}TiO_3$–$K_{1/2}Bi_{1/2}TiO_3$ ceramics. *Phys. Rev. B.*, 2013, **87**, 024113.
120. Goetzee-Barral, A. J., Usher, T. M., Stevenson, T. J., Jones, J. L., Levin, I., Brown, A. P. and Bell, A. J., Electric field dependent local structure of $(K_xNa_{1–x})_{0.5}Bi_{0.5}TiO_3$. *Phys. Rev. B*, 2017, **96**, 014118.
121. Zhang, S., Shrout, T. R., Nagata, H., Hiruma, Y. and Takenaka, T., Piezoelectric properties in $(K_{0.5}Bi_{0.5})TiO_3$–$(Na_{0.5}Bi_{0.5})TiO_3$–$BaTiO_3$ lead-free ceramics. *IEEE Trans. Ultrason. Ferroelectr. Freq. Control.*, 2007, **54**, 910–917.
122. Elkechai, O., Manier, M. and Mercurio, J. P., $Na_{0.5}Bi_{0.5}TiO_3$–$K_{0.5}Bi_{0.5}TiO_3$ (NBT–KBT) system: A structural and electrical study. *Phys. Status Solidi Appl. Res.*, 1996, **157**, 499–506.
123. Xie, H., Jin, L., Shen, D., Wang, X. and Shen, G., Morphotropic phase boundary, segregation effect and crystal growth in the NBT–KBT system. *J. Cryst. Growth.*, 2009, **311**, 3626–3630.
124. Zhang, Y. R., Li, J. F. and Zhang, B. P., Enhancing electrical properties in NBT–KBT lead-free piezoelectric ceramics by optimizing sintering temperature. *J. Am. Ceram. Soc.*, 2008, **91**, 2716–2719.
125. Zhang, Y. R., Li, J. F., Zhang, B. P. and Peng, C. E., Piezoelectric and ferroelectric properties of Bi-compensated $(Bi_{1/2}Na_{1/2})TiO_3$–$(Bi_{1/2}K_{1/2})TiO_3$ lead-free piezoelectric ceramics. *J. Appl. Phys.*, 2008, **103**, 074109.
126. Moosavi, A., Bahrevar, M. A., Aghaei, A. R., Ramos, P., Algueró, M. and Amorín, H., High-field electromechanical response of $Bi_{0.5}Na_{0.5}TiO_3$–$Bi_{0.5}K_{0.5}TiO_3$ across its morphotropic phase boundary. *J. Phys. D. Appl. Phys.*, 2014, **47**, 055304.
127. Babu, M. V. G., Bagyalakshmi, B., Venkidu, L. and Sundarakannan, B., Grain size effect on structure and electrical properties of lead-free $Na_{0.4}K_{0.1}Bi_{0.5}TiO_3$ ceramics. *Ceram. Int.*, 2017, **43**, 12599–12604.
128. Rubavathi, P. E., Babu, M. V. G., Bagyalakshmi, B., Venkidu, L., Dhayanithi, D., Giridharan, N. V. and Sundarakannan, B., Impact of Ba/Ti ratio on the magnetic properties of $BaTiO_3$ ceramics. *Vacuum*, 2019, **159**, 374–378.
129. Babu, M. V. G., Kader, S. A., Muneeswaran, M., Giridharan, N. V., Padiyan, D. P. and Sundarakannan, B., Enhanced piezoelectric constant and remnant polarisation in K-compensated sodium potassium bismuth titanate. *Mater. Lett.*, 2015, **146**, 81–83.
130. Bagyalakshmi, B., Ren, Y. and Sundarakannan, B., Grain size induced monoclinic (*Cm*) to rhombohedral (*R*3*c*) transformation in sodium potassium bismuth titanate ceramics. *Scr. Mater.*, 2017, **141**, 67–71.
131. Rao, B. N., Senyshyn, A., Olivi, L., Sathe, V. and Ranjan, R., Maintaining local displacive disorders in $Na_{0.5}Bi_{0.5}TiO_3$ piezoceramics by $K_{0.5}Bi_{0.5}TiO_3$ substitution. *J. Eur. Ceram. Soc.*, 2016, **36**, 1961–1972.
132. Adhikary, G. D., Khatua, D. K., Senyshyn, A. and Ranjan, R., Random lattice strain and its relaxation towards the morphotropic phase boundary of $Na_{0.5}Bi_{0.5}TiO_3$-based piezoelectrics: Impact on the structural and ferroelectric properties. *Phys. Rev. B.*, 2019, **99**, 174112.
133. Adhikary, G. D., Khatua, D. K., Senyshyn, A. and Ranjan, R., Long-period structural modulation on the global length scale as the characteristic feature of the morphotropic phase boundaries in the $Na_{0.5}Bi_{0.5}TiO_3$ based lead-free piezoelectrics. *Acta Mater.*, 2019, **164**, 749–760.
134. Adhikary, G. D. *et al.*, Increasing intervention of nonferroelectric distortion and weakening of ferroelectricity at the morphotropic phase boundary in $Na_{0.5}Bi_{0.5}TiO_3$−$BaTiO_3$. *Phys. Rev. B.*, 2019, **100**, 134111.
135. Otonicar, M., Park, J., Logar, M., Esteves, G., Jones, J. L. and Jancar, B., External-field-induced crystal structure and domain texture in $(1–x)Na_{0.5}Bi_{0.5}TiO_3$–$xK_{0.5}Bi_{0.5}TiO_3$ piezoceramics. *Acta Mater.*, 2017, **127**, 319–331.
136. Martin, A., Uršič, H., Rojac, T. and Webber, K. G., Direct observation of the stress-induced domain structure in lead-free $(Na_{1/2}Bi_{1/2})TiO_3$-based ceramics. *Appl. Phys. Lett.*, 2019, **114**, 052901.
137. Zhang, S. T., Kounga, A. B., Jo, W., Jamin, C., Seifert, K., Granzow, T., Rödel, J. and Damjanovic, D., High-strain lead-free antiferroelectric electrostrictors. *Adv. Mater.*, 2009, **21**, 4716–4720.
138. Malik, R. A., Kang, J. K., Hussain, A., Ahn, C. W., Han, H. S. and Lee, J. S., High strain in lead-free Nb-doped $Bi_{1/2}(Na_{0.84}K_{0.16})_{1/2}TiO_3$–$SrTiO_3$ incipient piezoelectric ceramics. *Appl. Phys. Express*, 2014, **7**, 061502.
139. Maurya, D., Zhou, Y., Wang, Y., Yan, Y., Li, J., Viehland, D. and Priya, S., Giant strain with ultra-low hysteresis and high temperature stability in grain oriented lead-free $K_{0.5}Bi_{0.5}TiO_3$–$BaTiO_3$–$Na_{0.5}Bi_{0.5}TiO_3$ piezoelectric materials. *Sci. Rep.*, 2015, **5**, 8595.
140. Singh, A. and Chatterjee, R., 0.40% bipolar strain in lead free BNT–KNN system modified with Li, Ta and Sb. *J. Am. Ceram. Soc.*, 2013, **96**, 509–512.
141. Weyland, F., Acosta, M., Koruza, J., Breckner, P., Rödel, J. and Novak, N., Criticality: concept to enhance the piezoelectric and electrocaloric properties of ferroelectrics. *Adv. Functional Mater.*, 2016, **26**, 7326–7333.
142. Hiruma, Y., Imai, Y., Watanabe, Y., Nagata, H. and Takenaka, T., Large electrostrain near the phase transition temperature of $(Bi_{0.5}Na_{0.5})TiO_3$–$SrTiO_3$ ferroelectric ceramics. *Appl. Phys. Lett.*, 2008, **92**, 262904.
143. Hiruma, Y., Nagata, H. and Takenaka, T., Thermal depoling process and piezoelectric properties of bismuth sodium titanate ceramics. *J. Appl. Phys.*, 2009, **105**, 084112.

144. Aksel, E., Forrester, J. S., Kowalski, B., Deluca, M., Damjanovic, D. and Jones, J. L., Structure and properties of Fe-modified $Na_{0.5}Bi_{0.5}TiO_3$ at ambient and elevated temperature. *Phys. Rev. B.*, 2012, **85**, 024121.
145. Anthoniappen, J., Tu, C. S., Chen, C. S., Chen, P. Y. and Idzerda, Y. U., Dielectric, ferroelectric, and depolarization properties of B-site manganese-doped $0.925(Bi_{0.5}Na_{0.5})TiO_3$–$0.075BaTiO_3$ solid solutions. *Ceram. Int.*, 2016, **42**, 8402–8408.
146. Mahajan, A., Zhang, H., Wu, J., Ramana, E. V., Reece, M. J. and Yan, H., Effect of phase transitions on thermal depoling in lead-free $0.94(Bi_{0.5}Na_{0.5}TiO_3)$–$0.06(BaTiO_3)$ based piezoelectrics. *J. Phys. Chem. C.*, 2017, **121**, 5709–5718.
147. Xu, Q., Huang, Y. H., Chen, M., Chen, W., Kim, B. H. and Ahn, B. K., Effect of bismuth deficiency on structure and electrical properties of $(Na_{0.5}Bi_{0.5})_{0.93}Ba_{0.07}TiO_3$ ceramics. *J. Phys. Chem. Solids*, 2008, **69**, 1996–2003.
148. Zhang, J. *et al.*, Semiconductor/relaxor 0–3 type composites without thermal depolarization in $Bi_{0.5}Na_{0.5}TiO_3$-based lead-free piezoceramics. *Nat. Commun.*, 2015, **6**, 6615.
149. Riemer, L. M. *et al.*, Stress-induced phase transition in lead-free relaxor ferroelectric composites. *Acta Mater.*, 2017, **136**, 271–280.
150. Li, L., Zhu, M., Zhou, K., Wei, Q., Zheng, M. and Hou, Y., Delayed thermal depolarization of $Bi_{0.5}Na_{0.5}TiO_3$–$BaTiO_3$ by doping acceptor Zn^{2+} with large ionic polarizability. *J. Appl. Phys.*, 2017, **122**, 204104.

ACKNOWLEDGEMENTS. R.R. thanks the Science and Engineering Research Board (SERB) of the Department of Science and Technology, Govt of India for financial support (Grant No. EMR/2016/001457); Council of Scientific and Industrial Research, and the IISc for supporting research on piezoceramics.

Received 2 January 2020; accepted 24 January 2020

doi: 10.18520/cs/v118/i10/1507-1519

.